Available online at www.sciencedirect.com

ScienceDirect

Ceramics International 40 (2014) 3721–3729

CERAMICS INTERNATIONAL

www.elsevier.com/locate/ceramint

Preparation of nanostructured YSZ granules by the spray drying method

Mohammad Reza Loghman-Estarki[a,c,*], Mousa Pourbafrany[b], Reza Shoja Razavi[b], Hossein Edris[a], Saeed Reza Bakhshi[b], Mohammad Erfanmanesh[b], Hossein Jamali[b], Seyed Naveed Hosseini[a], Morteza Hajizadeh-Oghaz[b]

[a]*Department of Materials Engineering, Isfahan University of Technology, P.O. Box. 84156-83111, Isfahan, Islamic Republic of Iran*
[b]*Department of Materials Engineering, Malek Ashtar University of Technology, Isfahan, Shahin-shahr, Islamic Republic of Iran*
[c]*Young Researchers and Elite Club, Kashan Branch, Islamic Azad University, Kashan, Iran*

Received 1 August 2013; received in revised form 10 September 2013; accepted 11 September 2013
Available online 16 October 2013

Abstract

The suspensions of nanosized YSZ powder with different binder (polyvinyl alcohol, PVA) contents were agglomerated into plasma sprayable feedstocks. The agglomeration was performed by the spray drying method. Two types of morphologies (spherical and non-spherical) were obtained after spray drying of the ball milled and non-ball milled nanopowders. The suitable granules size distributions (25–150 μm, average size = 45 ± 3 μm) with good apparent density (before calcination treatment = 800 kg/m^3 and after calcination = 900 kg/m^3) and flowability (before calcination = 0.31 g/s and after calcination = 0.41 g/s) for plasma spraying were obtained with 5 wt% PVA and calcination temperature up to 800 °C. Finally, the correlation between the granules shape and the resulting coating porosity and thermal insulation capability was investigated.

Keywords: Granules; Agglomerate; Nanostructure; Spray drying

1. Introduction

Ceramic powders are widely used in thermal spray to elaborate coatings with defined characteristics, such as thermal barriers. Thermal Barrier Coatings (TBCs) consist of a ceramic top coat made of yttria partially stabilized zirconia (YSZ), which is deposited over a metallic bond coat and used in aircraft turbine engines for thermal insulation in hot sections. Their thermal properties are closely related to the microstructure of the ceramic top coat [1–4], which is, in turn, influenced by the ceramic powder morphology. Handling dry nanosized powders is not only a potential health hazard, but also a technical challenge because of the inherent tendency of fine particles to form cohesive powder assemblies that contain hard agglomerates with a poor flowability [5]. Various methods have been employed for the fabrication of plasma sprayable nanostructured feeds (agglomerates particles or granules). The commonly used ceramic powders in plasma spraying are obtained by fusing and crushing, by the sol–gel method or by the spray drying process (SDP) [5–8]. Of all the above processes, the SDP method shows some advantages due to a spherical morphology and good flowability [5]. The SD method is routinely used as a spray granulation from slurries to obtain powder with various morphologies, depending on operating parameters and suspension formulation.

Most studies [9–11] using nanostructured spray-dried feedstock only mention the agglomeration process without providing any details on the nanoparticle suspension preparation, spray drying operation, or thermal treatment of the resulting agglomerates. In the present report, the agglomeration process was described in more details. Furthermore, the correlation between agglomeration process variables, agglomerate characteristics, and coating microstructure and properties was explained. The 7 wt% Y_2O_3 doped ZrO_2, named 7YSZ, and

*Corresponding author at: Department of Materials Engineering, Isfahan University of Technology, P.O. Box. 84156-83111, Isfahan, Islamic Republic of Iran. Tel.: +98 312 5225041; fax: +98 312 5228530.
E-mail addresses: mr.loghman@ma.iut.ac.ir, loghman57@gmail.com (M.R. Loghman-Estarki).

0272-8842/$ - see front matter © 2013 Elsevier Ltd and Techna Group S.r.l. All rights reserved.
http://dx.doi.org/10.1016/j.ceramint.2013.09.050

nanoparticles were used to obtain granules with a suitable density (close to 1000 kg/m^3) [12,13] and flowability (close to 0.4–0.5 g/s) [12,13] for plasma spraying via varying PVA content and calcination treatment technology. The study also addressed the correlation between the feedstock agglomerates with the resulting coating microstructure and porosity.

2. Experimental procedure

The partially stabilized zirconia nanopowder containing 7 wt% yttria was synthesized in large scale by the polymeric route as mentioned in Ref. [1]. The YSZ nanopowders were put into the ball milling (Retsch PM 100, Germany), which contained zirconia based balls (balls weight to powder was 10:1, the diameter of the zirconia milling balls was 5 mm). After 2 h ball milling, a typical mixture of 180 ml deionized water, 20 g YSZ nanopowders and 5 wt% binder (PVA, molecular weight ~10,000, Merck Co.) was stirred homogenously for 2 h. Some experiments were also done with different binder contents. According to the parameters in Table 1, the spray drying (spray dryer, Malek Ashtar Co., Iran) of suspensions was performed.

According to the ASTM nos. B0212-99 and B 213–03 [14], the evaluation of apparent density and flow rate of granules was performed, respectively. The viscosity of the suspensions was measured using a Krebs stormer viscometer (Max Techniques Co., Canada). The crystalline phases were obtained by the X-ray diffraction technique (Rigaku D-max C III, Philips, Holland) using Cu Kα radiation. A field-emission scanning electron microscope (FESEM) was obtained on S-4160 (Hitachi Ltd., Japan) and Philips (Holland Co.). The granule size distribution was measured by sieving it with different meshes and SEM analyses. Thermal barrier coatings, composed of a bond coating and a top coating, were air-plasma-sprayed on a Ni-based superalloy (Inconel 738, Ni–15Cr–8.5Co) substrate. The substrate geometry was a square of 10×10 mm^2 surface area with 10 mm thickness. Prior to the spraying process, the substrates were cleaned by absolute ethyl alcohol in an ultrasonic set. The substrates were then grit blasted by alumina particles with the size of 125 μm. Subsequently, the substrates were placed into the air plasma spray (APS) system (Switzerland PT Corporation, Plasma-Technik A3000S) for overlaying with NiCrAlY (Ni–22Cr–10Al–1Y, wt%) bond coating. Nanostructured 7YSZ was sprayed onto as sprayed bond coat specimen by an APS system. The APS parameters for depositing bond coat and top coat and their thickness are given in Table 2. The thermal insulation capability test was performed according to Ref. [8]. Thermal diffusivities of APS nanocoating was determined by Xenon flash analysis (XFA, Linesis model, Germany).

Coating void contents and semi-molten particle fractions were measured on the cross-sectional coating areas by the image analysis (Image pro-Plus Bethesada MD, USA) of the micrographs obtained by a scanning electron microscope (Philips, Holland) at 500 and 1000 × magnifications. Averages of seven images, randomly located across the sample, were analyzed for each sample in order to obtain a representative scan of the whole cross-sectional area.

3. Results and discussion

3.1. Characterization of YSZ nanopowder

Fig. 1a shows the SEM image illustrating the morphology of the YSZ nanopowder obtained from the polymeric sol–gel method. This sample consists of relatively compact large particles that show flat faces and angular edges. This typical morphology was similar to other studies in the literature [1,15–19]. High magnifications of these big facets (Fig. 1b) show that they consist of nanometric YSZ nanoparticles. TEM picture in Fig. 1c shows that the as-prepared samples consist of crystallites with a size between 30 and 50 nm. According to XRD pattern (Fig. 1d), YSZ nanopowders show a pure tetragonal phase with cell parameters $a=b=0.36290$ nm and $c=0.51282$ nm.

3.2. Spray drying and calcination process

3.2.1. Spray drying

In order to survey the effect of binder concentration on the morphology of as-prepared granules, the FESEM image was taken from them. Fig. 2 shows FESEM micrographs of spray-dried powders obtained from 0–15 wt% binders in suspensions.

Table 1
The parameters of spray drying.

Inlet temp. (°C)	Output temp. (°C)	Rotate speed of atomizer (rpm)	Type of atomizer	Rate of air flow (l/h)	Feedstock flow (kg/h)
225–235	135–140	17,000	Disk-like	4.4–4.6	1.0–1.2

Table 2
Plasma spraying parameters and coating thickness.

Type of material	Thickness (μm)	Current (A), voltage (V)	Primary gas (Ar), secondary gas (H_2) (SLPM[a])	Carrier gas (Ar) (SLPM[a])	Spray distance (mm), spray angle (deg)	Powder feed rate (g/min)	Nozzle, injector diameter (mm)
7YSZ	~220–250	600, 72	35, 10	3.5	120, 90	18	6, 1.8
NiCrAlY	120–140	600, 75	65, 14	2.3	120, 90	40	6, 2.5

[a]Standard liter per minute.

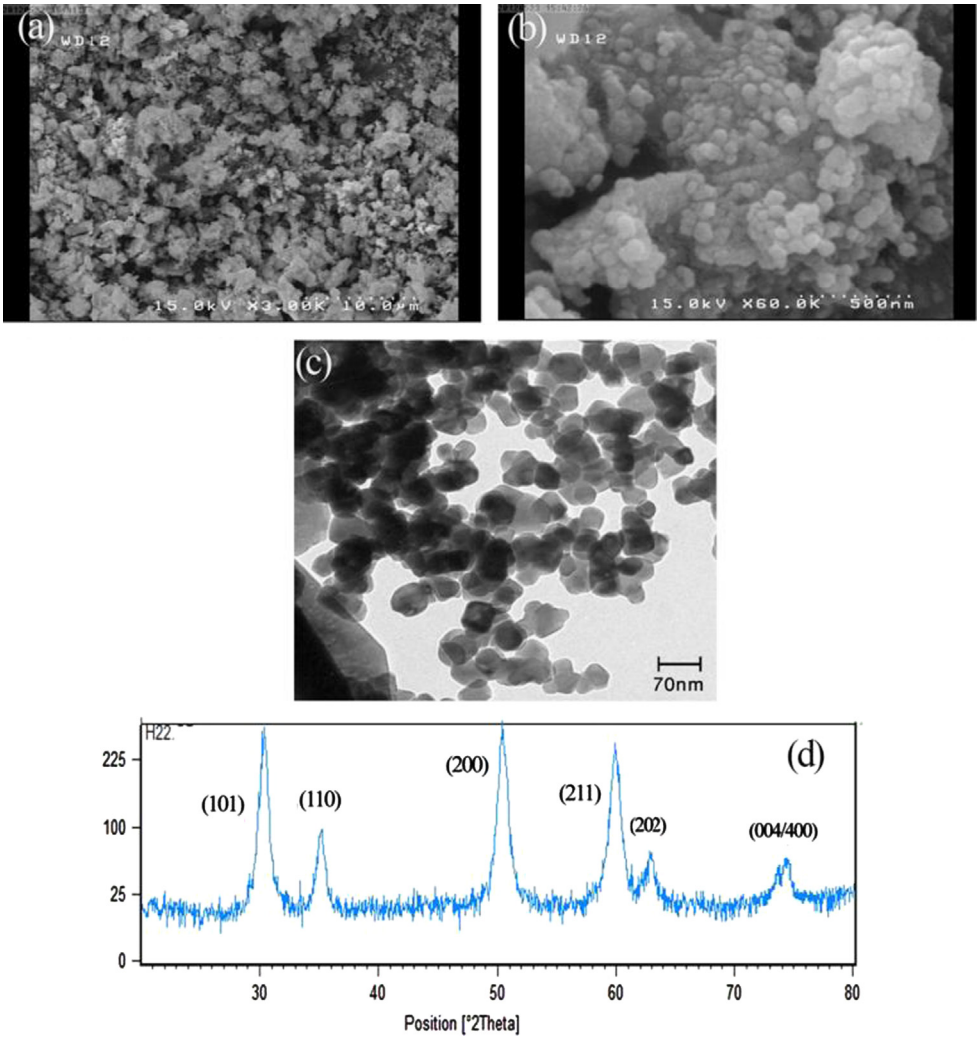

Fig. 1. SEM image with different magnifications (a) and (b), TEM images (c), and XRD patterns (d) of YSZ nanopowder prepared by polymeric route.

Fig. 2a displays particles morphology of YSZ suspension without binder, after spray drying process. According to these figures, granules are hollow (labeled with red line). Furthermore, due to the absence of binder in suspension, there are a lot of non-spherical particles (big facets) in Fig. 2a. Most granules (Fig. 2b–d) of YSZ nanopowders exhibit the typical semispherical shape with smooth surfaces of spray-dried agglomerates. However, the 15 wt% binder is much more homogeneous since the granules display a more spherical profile and uniform sizes. In addition, some deformed granules, in the presence of large facets, are visible in 15 wt% samples (Fig. 2d). This heterogeneity can be attributed to liquid-phase separation during the spray-drying operation, possibly due to some surface tension modifier incorporated into the suspension. Higher magnification of the solid areas (Fig. 2e) of the agglomerates of all powders reveals that the granules are porous. They are formed by the agglomeration of individual nanoparticles (30–50 nm). According to Fig. 2e, the diameter of nanoparticles was not changed in comparison with the original YSZ nanopowder (Fig. 2a and b).

Agglomerate apparent specific mass (Table 3) was determined for 5–15 wt% binder, because the heterogeneity of the 0 wt% binder did not allow the assumption of uniform granule size distribution to be fulfilled. The value obtained for 5 wt% binder (830 kg/m^3) was higher than the other granules. Furthermore, adding a binder to these slurries changed their viscosity and thus, their granule size distribution, as reported in Table 3. According to this table, 5 wt% PVA content had a suitable size distribution (4%: $d < 20$ μm, 75%: 20 μm $< d <$ 105 μm and 21%: 105 μm $< d <$ 150 μm) for plasma spraying than the other granules. Laser particle size analyzer (Appendix A) was also confirmed that the majority of particle in the sample prepared with 20 wt. % PVA, have sizes larger than 100 micron. However, for other sample, because of using ultrasonic wave for dispersing nanogranules in water medium, some granules was broken into nanoparticle. So, curve a-d in Appendix A, show in all sample, there is particle with size distribution lower than 1 μm.

The obtained different sizes of granules, with changing the PVA content, could be described in terms of the following empirical equation:

$$SMD = C\left(\frac{\rho_L^{0.25}\mu_L^{0.06}\sigma^{0.375}}{\rho_A^{0.375}}\right)\left(\frac{\dot{m}_L}{\dot{m}_L U_L + \dot{m}_A U_A}\right)^{0.55} \quad (1)$$

where SMD is the Sauter median diameter, C is a constant whose value depends on atomizer design; ρ, μ, σ, U and $\dot{m}$ are

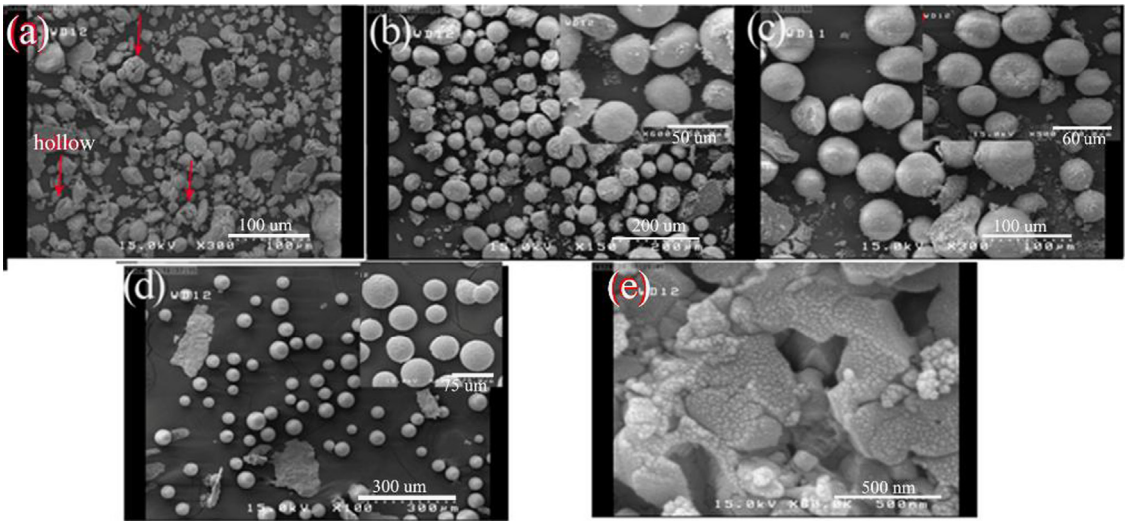

Fig. 2. FESEM micrographs of spray-dried powders obtained from different PVA contents (wt%) (a) 0, (b) 5, (c)10, and (d) and (e) 15. (Insets are high magnifications of each SEM image.) (For interpretation of the references to color in this figure, the reader is referred to the web version of this article.)

Table 3
The correlation between binder content in the suspension and density and flowability of granules.

Binder content (wt%)	Granule size distribution $d < 20$ μm, 20 μm $< d <$ 105 μm, 105 μm $< d <$ 150 μm	Average diameter (μm)	Flowability (g/s)	Viscosity (mPa s)	Density (before calcination treatment) (kg/m^3)
0	50%, 30%, 20%	40 ± 5	–	4	–
5	4%, 75%, 21%	45 ± 3	0.31	18	800
10	6%, 50%, 44%	50 ± 4	0.27	21	680
15	5%, 30%, 65%	70 ± 2	0.26	29.4	430

the density, the viscosity, the surface tension, the velocity and the flow rate of the liquid (L) or air (A) [20]. Upon increasing PVA content, the viscosity (μ parameter in Eq. (1), Table 1) of suspension was increased and then *SMD* became bigger than low PVA content. In the next section, it is described how the density of this granule can be improved by the calcination process.

In order to survey the effect of ball milling treatment on the morphologies of as-prepared granules, the slurry was prepared with non-ball milling YSZ nanopowders and 5 wt% PVA. Fig. 3b displays the particles morphology of YSZ suspension without ball milling treatment, after spray drying process. According to this figure, the untreated nanopowders resulted in irregular non-spherical morphology with dimensions ranging from 30 μm to 100 μm (Fig. 3b). The SEM images (Fig. 3c) of ball milled YSZ nanopowder, before spray drying process, show that big agglomerates in Fig. 3a were broken to small ones. So, after spray drying of this powder, spherical granules (Fig. 3d) were obtained. However, irregular and angular morphologies of Fig. 3b resulted from original angular nature of as-obtained YSZ nanopowders (Fig. 3a) prepared with the polymeric sol–gel method [15,21–23]. However, during spray drying of non-ball milled YSZ nanopowders, the surface tension pulled some droplets into a semi-sphere morphology (Fig. 3b).

Furthermore, the agglomerate apparent specific mass of spherical (SD1, the granules obtained by spray-drying the milled nanopowders) and irregular non-spherical granules (SD2, the one obtained by spray-drying the non-milled nanopowders) was determined. The value of agglomerate apparent specific mass of the SD2 (non-spherical granules, 830 kg/m^3) sample was higher than those of the SD1 (spherical granules, 800 kg/m^3) sample. However, the flowability of the SD1 (0.31 g/s) sample was higher than those of SD2 (0.24 g/s) sample due to their spherical morphology and smooth surface. Researchers have reported [20] that spray-dried powder with apparent specific mass > 1700 kg/m^3 and mean particle size > 20 μm can be directly processed for plasma spray coating without further densification. Another paper states that the apparent specific mass of the agglomerates of APS spray-dried powders can range widely from less than 1000 kg/m^3 to 2000 kg/m^3 [12,13]. In the next section, it is described how the apparent density of this granule can be improved by calcination (heat treatment) process. Indeed, the feedstocks do not meet the demands for the plasma spraying method after granulation process.

3.2.2. Calcining process

In order to increase the density and eliminate all organic additives, the granulated particles obtained from the spray drying process were calcined at a high temperature. The thermo-gravimetric analysis (TGA) was used to assign calcinations temperature, as shown in Fig. 4. In Fig. 4a, the mass loss before 300 °C and 300–570 °C is due to the

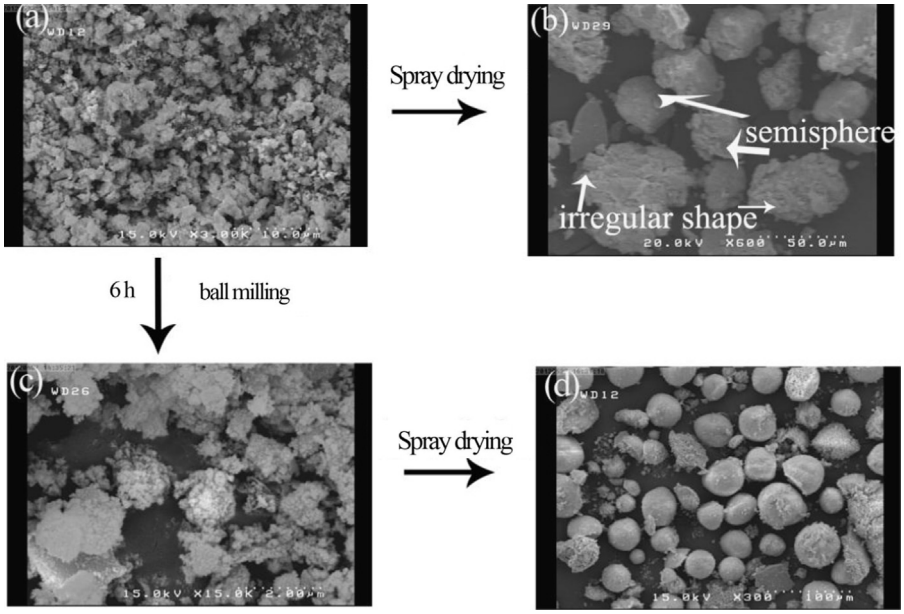

Fig. 3. SEM images of YSZ (a) nanopowder before ball milling, (b) granules prepared from non-ball milled nanopowder, (c) nanopowder after ball-milling process and (d) granules prepared from ball milled nanopowder.

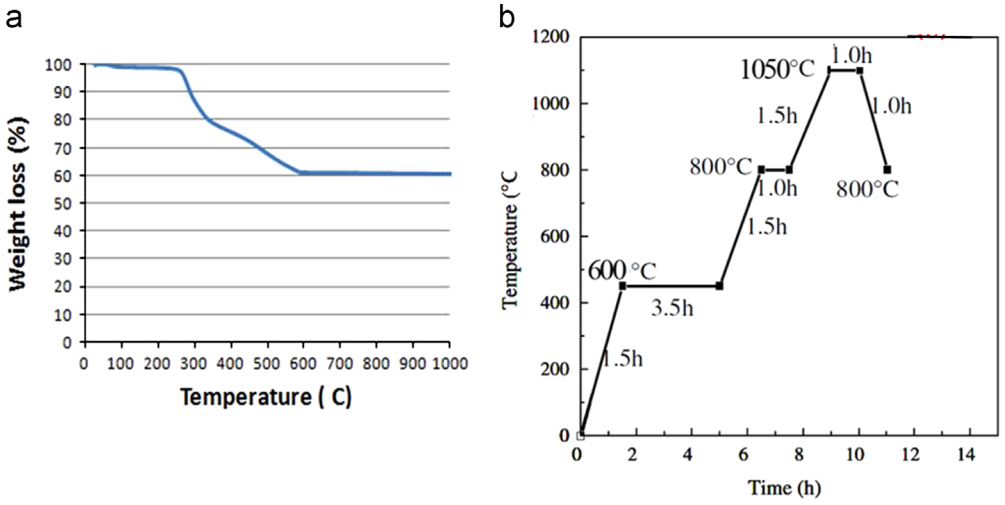

Fig. 4. TGA of granules prepared with 5 wt% binder (a) and (b) heat treatment process.

evaporation of deionized water and decomposition of PVA (polyvinyl alcohol), respectively. The heating rate should be slow at low sintering temperature, making the deionized water and polymer evaporate and volatilize fully. However, at high temperature stage, the heating rate is high, preventing the growth of nanogranules (Fig. 4b). After sintering at 1050 °C, the apparent density of SD1 and SD2 granules was increased from 800 and 830 kg/m^3 to 910 and 1010 kg/m^3, respectively. It was due to the cracks in the particles that were decreased at low heating rate and the adhesive strength of agglomerated particles was strengthened by the self-assembly of nanoparticles and grain growth (Fig. 5a–d) [12,13]. The particle growth was caused by increasing calcination temperature from 800 to 1050 °C. Fig. 5a shows the particle morphology of YSZ at calcination process up to 800 °C. Compared with the sintering at 1050 °C (Fig. 5c and d), the particle size on the granules was lower (below 70 nm) than the other one. The particle surface was relatively smooth, and the flowability was 0.41 g/s. However, at calcination temperature equals to 800 °C, the apparent density of SD1 granules increased from 800 kg/m^3 to 900 kg/m^3. Fig. 5c and d shows the particle morphology after sintering at 1050 °C. The surface of powders was very coarse and particle size was equivalent to the powders without sintering. The rough powders consisted of some submicron crystal grains (90–150 nm). The organic PVA was decomposed and volatilized, making the particles surface rough.

The granules calcined at 1050 °C had a good density but the grain sizes were grown more than 100 nm. So, to have granules with grain size less than 100 nm and appropriate density, the calcination temperature up to 800 °C was selected. So, this calcination temperature was applied for SD2 (non-ball milled one) granules. The SD2 granules, at this calcination

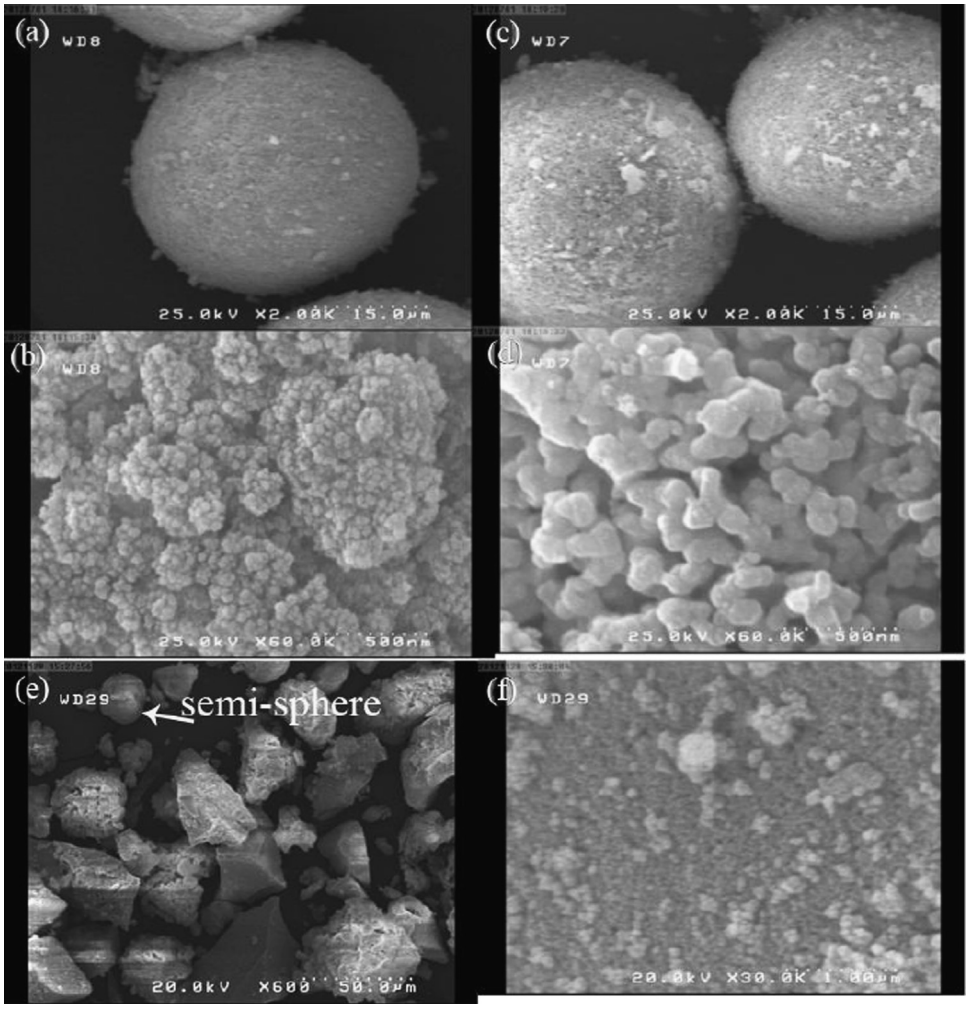

Fig. 5. SEM images of SD1 granules after heat treatment up to 800 °C (a) and (b), and 1050 °C (c) and (d). SD2 (e) and (f) after heat treatment up to 800 °C.

temperature, showed low grain growth as compared to SD1 (Fig. 5d and e). The apparent density and flowability of these granules were increased from 830 kg/m^3 and 0.24 g/s to 930 kg/m^3 and 0.32 g/s, respectively.

3.3. APS coatings from agglomerated feedstock

The coatings were obtained from the following spray-dried feedstocks: ball milled SD granules (SD1 – 800 °C, spherical) and non-ball milled (SD2 – 800 °C, non-spherical) ones. Figs. 6 and 7 show FESEM micrographs of the fractured and polished cross-section of coatings obtained from SD1 and SD2 powders at different magnifications, respectively. The coatings displayed the typical microstructure of APS coatings deposited from nanostructured powders, as used here [9]. The literature indicates that such coating microstructures basically comprise two clearly differentiated zones, yielding a two-scale structure [10,22]. One coating region, which is completely melted (marked M in Fig. 6), mainly consists of submicrometre-sized grains of YSZ. The other one, which is only partly melted (marked PM), largely retains the microstructure of the starting powder; thus, it is principally made up of nanometer-sized grains of YSZ. The particle size of this splat-quenched YSZ is extremely small (20–70 nm). No significant differences were observed between the micrographs of both coatings. The contribution of this two-scale coating structure to the enhancement of coating properties can be compared to conventional micrometer-sized coatings, as clearly shown elsewhere [10,22]. However, most studies focus on the impact of plasma spraying variables on the amount of the preserved nanostructure area, while the role of granulated feedstock has rarely been addressed [6,7]. In view of the above, the total void content of the coatings, as well as the amount of semi-molten areas (PM area), was estimated by image analysis at 500 and 1000 × magnifications. These magnifications enable void content and semi-molten nanozone areas to be estimated for comparative purposes. However, voids cannot be readily distinguished from semi-molten areas because both areas are detected as black particles. To perform this identification, the binary images of the sample were first obtained in black and white colors. Subsequently, the assignment of the distribution of black areas was made as follows: voids + semi-melted area (total area of black particles), voids (total area of black particles − areas of black particles with a surface area greater than 100 μm^2) and semi-melted areas (area of black particles with a surface area greater than 100 μm^2).

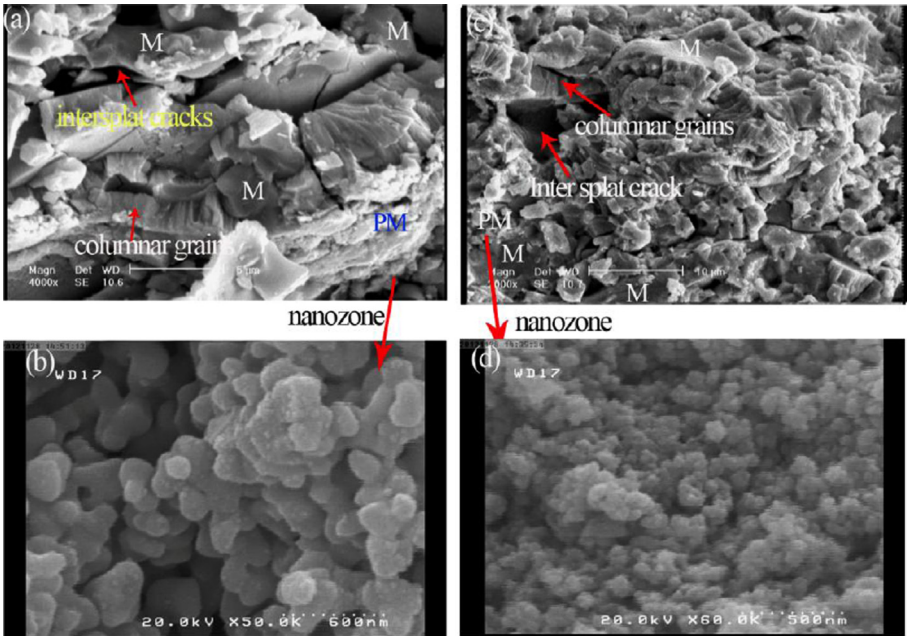

Fig. 6. SEM micrographs of fracture sections of YSZ APS coatings with different magnifications which were plasma sprayed from SD1 (spherical) (a) and (b), and SD2 (non-spherical) (c) and (d) powder. (M = melted area, PM = partially melted zone).

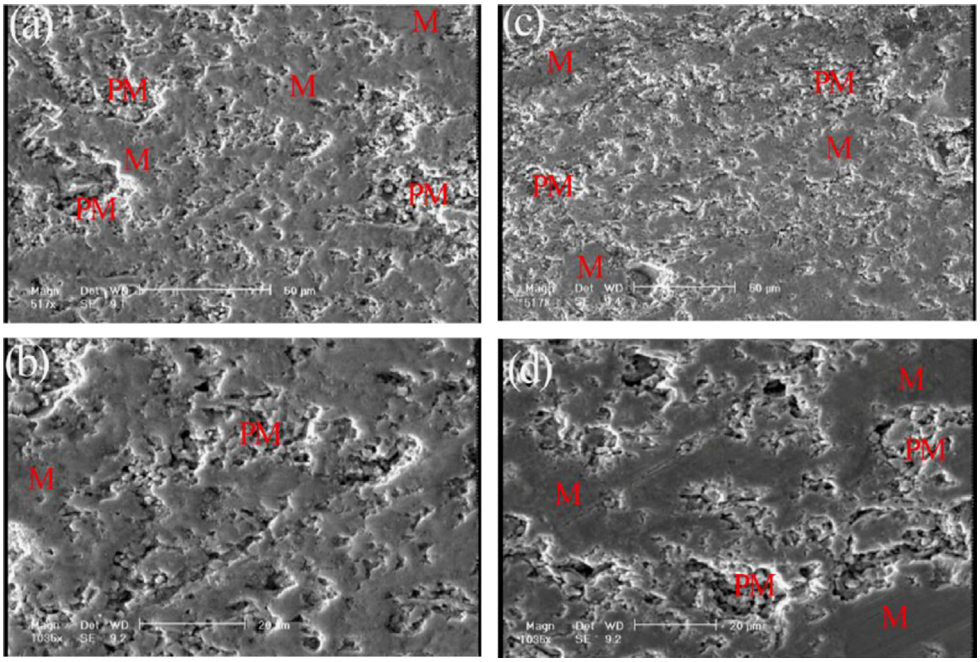

Fig. 7. SEM images of cross-section of YSZ APS coating with different magnifications which were plasma sprayed from SD1(spherical) (a) and (b), and SD2(non-spherical) (c) and (d) powder. (M = melted area, PM = partially melted zone).

The 100 μm^2 threshold for the semi-molten areas was assigned after microscopic observation of many of these areas. The void content data at 500 × magnifications are detailed in Table 4. The results at 1000 × magnifications were very similar to those obtained at 500 × magnifications, but a better differentiation was observed between the voids and the semi-molten areas at 1000 × magnifications.

Table 4
Voids and partially melted areas of APS coatings determined by the image analysis.

Coating sample	Voids + PM areas (%)	Voids (%)	PM areas (%)
SD1 (spherical)	34 ± 4	5 ± 1	29 ± 3
SD2 (non-spherical)	27 ± 3	10 ± 2	17 ± 4

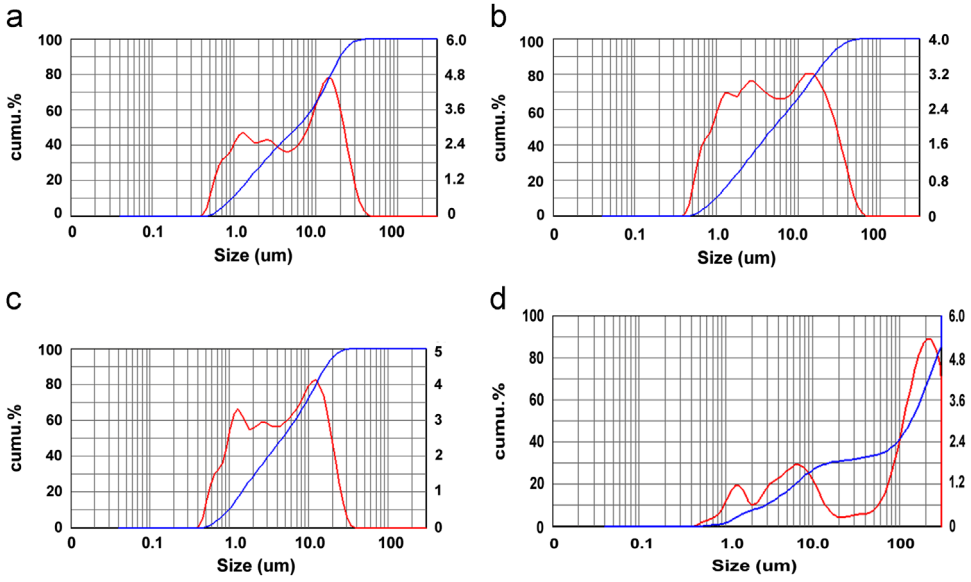

Fig. A1. Laser particle size analyzer of nanogranules obtained by different PVA contents (a) 0, (b) 5 and (c) 10 (d) 20 PVA (dispersed in water medium by ultrasonic treatment).

Despite their relative inaccuracy, these data suggest interesting conclusions. First, before spray drying, ball-milling of nanopowders appears to be an effective way of reducing coating void content. Second, non-spherical granulates obtained from non-ball milled nanopowder seem to lead to less porous coatings, in which the amount of semi-molten areas is also reduced. It is due to the heat transfer from plasma to the nanoparticles, which is completely different in nanostructured spherical agglomerates when compared with irregular dense granules. This is because heat transfer from the plasma plume to the inner core of the dense agglomerates [9,22], making it more difficult for them to melt completely (the SD2 granules are denser than the SD1 ones). This condition can lead to different partially melting states in the APS coating of SD1 and SD2 samples (Table 4). Furthermore, thermal insulation capability of TBC coating obtained by spherical granules was 11 °C higher than non-spherical one. These findings show that controlling feedstock characteristics affect the amount of porosity and thermal properties of TBC coating. Moreover, thermal diffusivities of APS nanocoating produced from commercial 7YSZ (Nanox-S4007 powder, spherical granules), 7YSZ (synthesized by the sol–gel method, non-spherical granules) and scandia, yttria stabilized zirconia (SYSZ, synthesized by the sol–gel method [18], non-spherical granules) were obtained as 0.0157 cm^2/s, 0.0175 cm^2/s and 0.0193 cm^2/s, respectively. Furthermore, with removing impurity such as Fe, Al, Cr, thermal insulation value of purified SYSZ nanocoating in Ref. 21 was improved from 56 °C [21] to 92 °C.

4. Conclusions

Spherical and irregular morphologies were obtained from spray drying of ball milled and non-ball milled YSZ suspensions, respectively. Furthermore, the added amount of PVA was optimized with respect to the flowability and density properties. The spherical granules with good flowability and density properties were obtained with 5 wt% PVA. When the powder was sintered in a furnace (800 °C), lower grain growth and approximately no shape variations were noticed as compared with the one sintered at 1050 °C. In this temperature (1050 °C), granules tended to crystal growth more than 100 nm. Finally, spherical granules resulted in more porous coating and higher thermal insulation capability than dense irregular granules.

Appendix A

See Appendix Fig. A1.

References

[1] M. Salavati-Niasari, M. Dadkhah, F. Davar, Pure cubic ZrO_2 nanoparticles by thermolysis of a new precursor, Polyhedron 28 (2009) 3005–3009.
[2] M. Salavati-Niasari, M. Dadkhah, F. Davar, Synthesis and characterization of pure cubic zirconium oxide nanocrystals by decomposition of bis-aqua, tris-acetylacetonato zirconium(IV) nitrate as new precursor complex, Inorg. Chim. Acta 362 (2009) 3969–3974.
[3] M. Salavati-Niasari, M. Dadkhah, M.R. Nourani, A.A. Fazl, Synthesis and Characterization of single-phase cubic ZrO_2 spherical nanocrystals by decomposition route, J. Cluster Sci. 23 (2012) 1011–1017.
[4] M.R. Loghman-Estarki, R. Shoja Razavi, H. Edrsi, et al., Life time of new SYSZ thermal barrier coatings produced by plasma spraying method under thermal shock test and high temperature treatment, Ceram. Int. 23 (2013) http://dx.doi.org/10.1016/j.ceramint.2013.07.023, in press.
[5] K. Masters, Drying of droplets/sprays, Spray Drying Hand Book, 4th ed., John Wiley & Sons, New York, 2001.
[6] X.J. Ning, C.X. Li, C.J. Li, G.J. Yang, Effect of powder structure on microstructure and electrical properties of plasma-sprayed 4.5 mol% YSZ coating, Vacuum 80 (2006) 1261–1265.
[7] A.J. Allen, G.G. Long, H. Boukari, J. Ilavsky, A. Kulkarni, S. Sampath, H. Herman, A.N. Goland, Microstructural characterization studies to relate the properties of thermal spray coatings to feedstock and spray conditions, Surf. Coat. Technol. 146 (2001) 544–550.

[8] W.B. Gong, C.K. Sha, D.Q. Sun, W.Q. Wang, Microstructures and thermal insulation capability of plasma-sprayed nanostructured ceria stabilized zirconia coatings, Surf. Coat. Technol. 201 (2006) 3109–3114.
[9] R.S. Lima, B.R. Marple, Thermal spray coatings engineered from nanostructured ceramic agglomerated powders for structural, thermal barrier and biomedical applications: a review, J. Therm. Spray Technol. 16 (2007) 40–46.
[10] P. Fauchais, G. Montavon, R.S. Lima, B.R. Marple, Engineering a new class of thermal spray nano-based microstructures from agglomerated nanostructured particle suspensions and solutions, J. Phys. D: Appl. Phys. 44 (2011) 093001–093054.
[11] S. Kamal, R. Jayaganthan, S. Prakash, Hot corrosion behavior of D-gun sprayed NiCoCrAlYTa coated superalloys at 900 °C in molten salt environment, Surf. Eng. 26 (2010) 453–462.
[12] E. Sánchez, A. Moreno, M. Vicent, M.D. Salvador, V. Bonache, E. Klyatskina, I. Santacruz, R. Moreno, Preparation and spray drying of Al_2O_3–TiO_2 nanoparticle suspensions to obtain nanostructured coatings by APS, Surf. Coat. Technol. 205 (2010) 987–994.
[13] Z. Pan, Y. Wang, X. Sun, Fabrication and characterization of spray dried Al_2O_3–ZrO_2–Y_2O_3 powders treated by calcining and plasma, Powder Technol. 212 (2011) 316–326.
[14] (a) ASTM B0212-99, Test Method for Apparent Density of Free-Flowing Metal Powders Using the Hall flowmeter funnel;
(b) ASTM B 213-03, Standard Test Method for Flow Rate of Metal Powders.
[15] M.R. Loghman-Estarki, R. ShojaRazavi, H. Edris, Synthesis of SYSZ nanocrystal via new wet chemistry method, Curr. Nanosci. 8 (2012) 767–782.
[16] W. Li, L. Gao, Nano ZrO_2–Y_2O_3 particles processing by heating of ethanol–aques salt solution, Ceram. Int. 27 (2001) 543–549.
[17] S. Zürcher, T. Graule, Influence of dispersant structure on the rheological properties of highly-concentrated zirconia dispersions, J. Eur. Ceram. Soc. 25 (2005) 863–869.
[18] M.R. Loghman-Estarki, R. Shoja Razavi, H. Edris, Large scale synthesis of tetragonal SYSZ nanopowders to obtain APS coating, Ceram. Int. *39* (2013) 7817–7829.
[19] M.R. Loghman-Estarki, M. Hajizadeh-Oghaz, R. Shoja Razavi, H. Edris, Comparative studies on synthesis of nanocrystalline Sc_2O_3–Y_2O_3 doped zirconia (SYDZ) and YSZ solid solution via modified and classic Pechini method, Cryst. Eng. Commun. 15 (2013) 5898–5923.
[20] X.Q. Cao, R. Vassen, S. Schwartz, W. Jungen, F. Tietz, D. Stöever, Spray-drying of ceramics for plasma-spray coating, J. Eur. Ceram. Soc 20 (2000) 2433–2439.
[21] M.R. Loghman-Estarki, R. Shoja Razavi, H. Edris, Spray drying of nanometric SYSZ powders to obtain plasma sprayable nanostructured granules, Ceram. Int. 39 (2013) 9447–9457.
[22] H. Jamali, R. Mozafarinia, R. Shoja Razavi, R. Ahmadi-Pidani, M.R. Loghman-Estarki, Fabrication and evaluation of plasma-sprayed nanostructured and conventional YSZ thermal barrier coatings, Curr. Nanosci. 8 (2012) 402–409.
[23] N. Mir, M. Salavati-Niasari, Preparation of YSZ nanoparticles by a two-step sol-gel method to Preparation of TiO_2 nanoparticles by a two-step sol-gel method, Mater. Res. Bull. 48 (2013) 1660–1667.